

This is the accepted manuscript made available via CHORUS, the article has been published as:

Three Pomerons versus D0 and TOTEM data

V. A. Petrov and A. Prokudin

Phys. Rev. D **87**, 036003 — Published 6 February 2013

DOI: [10.1103/PhysRevD.87.036003](https://doi.org/10.1103/PhysRevD.87.036003)

where the eikonal $\delta(s, b)$ is approximated by single-reggeon exchanges

$$\delta_{pp}^{\bar{p}p}(s, b) = \delta_{\mathbb{P}}^+(s, b) \mp \delta_{\mathbb{O}}^-(s, b) + \delta_f^+(s, b) \mp \delta_{\omega}^-(s, b). \quad (2)$$

We refer the reader to the original literature for details; let us simply recall that here $\delta_{\mathbb{P}}^+(s, b)$ is the Pomeron contributions and superscript ‘+’ denotes C-even trajectories (the Pomeron trajectories have quantum numbers $0^+ J^{++}$), while ‘-’ denotes C-odd trajectories. $\delta_{\mathbb{O}}^-(s, b)$ is the Odderon contribution (i.e. the C-odd partner of the Pomeron whose quantum numbers are $0^- J^{--}$); δ_f^+ and $\delta_{\omega}^-(s, b)$ are the contributions of secondary Reggeons, f as representative of the $C = +1$ families and ω of the $C = -1$.

This approximation for the eikonal is similar to the impact parameter approximation in quantum mechanics with single-reggeon exchanges in the role of potentials. Actually this assumption is generic for many models in the field. From the standpoint of the complex J -plane, the eikonal has to have not only Regge poles but, generally, more complicated singularities. Nonetheless, we believe that the pole approximation for the eikonal reasonably reflects the gross features of the diffractive hadron scattering. In our model we use linear trajectories and this could be justified if one considers only low- t region. Our linear Pomeron trajectories can go below the line $J = 1$ at sufficiently large $-t$, however, Regge trajectories in QCD are non-linear at negative t , see Refs. [40]. Pomeron trajectories most probably always lie higher than $J = 1$, see Ref. [41]. If there is a disagreement with data, we have to pay closer attention to such details.

As was said, the effective number of Pomerons was found to be three, and the pomeron contribution $\delta_{\mathbb{P}}^+(s, b)$ can be, accordingly, represented as the sum of three contributions:

$$\delta_{\mathbb{P}}^+(s, b) = \delta_{\mathbb{P}_1}^+(s, b) + \delta_{\mathbb{P}_2}^+(s, b) + \delta_{\mathbb{P}_3}^+(s, b), \quad (3)$$

each of those having a particular Regge trajectory. Other models include complicated form-factors [24] or a different type of singularity for the Pomeron [11].

Let us recall that if the form of Eq. (3) is indeed manifested in nature, then we expect to have particles lying on the corresponding trajectories. The model predicts $M_{glueball}^2 = 1.68, 3.05, 8.51$ (GeV^2) for $0^+ 2^{++}$ state. The trajectories from Ref. [1] are presented in Fig. 1. In fact one of the $0^+ 2^{++}$ candidates is situated very close to trajectory of \mathbb{P}_2 .

In Ref. [1] this three-component Pomeron model was successfully used for description of high energy pp and $\bar{p}p$ data in the region of large momentum transfers $0.01 \leq |t| \leq 14.5$ GeV^2 . In Ref. [2] the model was extended to the region of small momentum transfers $0 \leq |t| \leq 0.01$ GeV^2 . In order to do this we have to account for the Coulomb interaction. The standard way is to represent the whole scattering amplitude $T(s, t)$ which is dominated by the Coulomb force at low momentum transfers and by the hadronic force at higher momentum transfers as

$$T(s, t) = T^N(s, t) + e^{i\alpha\Phi} T^C(s, t), \quad (4)$$

where we normalize the scattering amplitude so that

$$\frac{d\sigma}{dt} = \frac{|T(s, t)|^2}{16\pi s^2}, \quad (5)$$

and the Born Coulomb amplitude for pp and $\bar{p}p$ scattering is

$$T^C(s, t) = \mp \frac{8\pi\alpha s}{|t|}. \quad (6)$$

The upper (lower) sign corresponds to the scattering of particles with the same (opposite) charges. $T^N(s, t)$ stands for purely strong interaction amplitude, and the phase Φ depends generally on energy, momentum transfer and on the properties of T^N . We considered three different forms of the phase Φ calculated earlier by West and Yennie [42], Cahn [43] and Selyugin [44] and showed in Ref. [2] that all three phases lead to a good description of the low- t data.

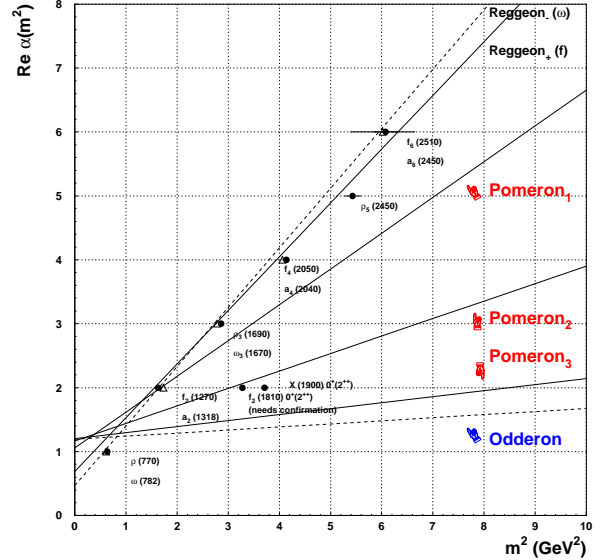


FIG. 1: Regge trajectories from Ref. [1].

In order to relate t - and b -spaces one proceeds via Fourier-Bessel transforms

$$\hat{f}(t) = 4\pi s \int_0^\infty db^2 J_0(b\sqrt{-t}) f(b) , \quad (7)$$

$$f(b) = \frac{1}{16\pi s} \int_{-\infty}^0 dt J_0(b\sqrt{-t}) \hat{f}(t) . \quad (8)$$

Crossing symmetry is restored by replacing $s \rightarrow se^{-i\pi/2}$. We introduce the dimensionless variable

$$\tilde{s} = \frac{s}{s_0} e^{-i\frac{\pi}{2}} , \quad s_0 = 1 \text{ (GeV}^2\text{)} , \quad (9)$$

in terms of which we give each $C+$ and $C-$ contribution with an appropriate signature factor in the form

$$\delta^\pm(s, b) = \mathcal{C} \frac{c}{s_0} \tilde{s}^{\alpha(0)-1} \frac{e^{-\frac{b^2}{\rho^2}}}{4\pi\rho^2} , \quad \text{with } \rho^2 = 4\alpha'(0) \ln \tilde{s} + r^2 , \quad (10)$$

where $\mathcal{C} = i$ for $C+$ and $\mathcal{C} = 1$ for $C-$.

For the cross-sections we use the following normalizations: Total and elastic cross-sections are normalized such that

$$\sigma_{tot} = \frac{1}{s} \Im m T(s, t=0), \quad \sigma_{elastic} = 4\pi \int_0^\infty db^2 |T(s, b)|^2 . \quad (11)$$

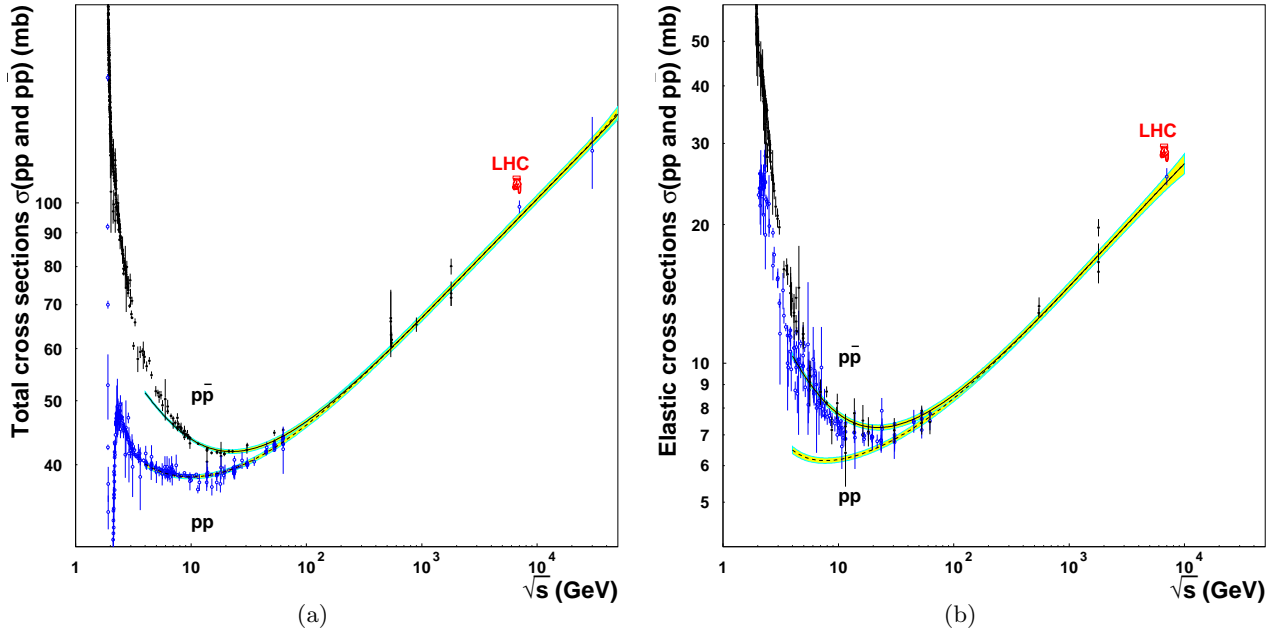


FIG. 2: Total (a) and elastic (b) cross sections for pp and $p\bar{p}$ scattering. The yellow band corresponds to the error propagation of parameter uncertainties of the model.

III. RESULTS AND DISCUSSIONS

In Ref. [1], the adjustable parameters were fitted over a set of 982 pp and $p\bar{p}$ data points [45] of both forward observables (total cross-sections σ_{tot} , and ρ , ratios of the real to the imaginary part of the amplitude) in the range $8 \leq \sqrt{s} \leq 1800$ GeV and angular distributions ($\frac{d\sigma}{dt}$) in the ranges $23 \leq \sqrt{s} \leq 1800$ GeV, $0.01 \leq |t| \leq 14$ GeV². A good $\chi^2/d.o.f. = 2.6$ (we did not consider systematic errors in normalizations of data sets and thus assumed that the

value of $\chi^2/d.o.f.$ to be satisfactory) was obtained and the parameters are given in Appendix A Table II. A set of the data including the Coulomb region which consists of 2158 points [45] was considered in Ref. [2] and it was shown that Coulomb-nuclear interference well described the data. We also found that the Coulomb phases from Ref. [43] and Ref. [44] gave a good account of the data in the lowest- t region.

The total and elastic cross sections are presented in Fig. 2. Note that in contrast to Ref. [1] we included the error corridor as explained in Appendix A. In Fig. 2 we also plot the experimental values of the total and elastic cross sections found by the TOTEM. As one can see, the model predictions are very close to the data. We show $p\bar{p}$ angular distributions over the full range of $|t|$ and in comparison with the DØ data at 1.96 TeV in Fig. 3. One can see that the data are predicted perfectly well by the model.

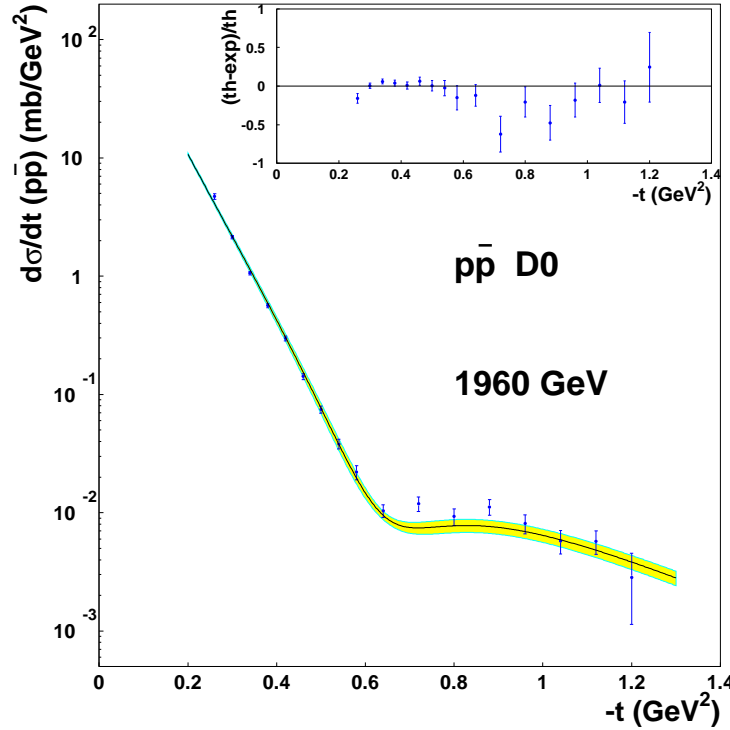


FIG. 3: Differential cross section for $p\bar{p}$ scattering at 1.96 TeV and comparison with the DØ data. The yellow band corresponds to the error propagation of parameter uncertainties of the model. The upper panel shows the variance of the model predictions and the data.

We show pp angular distributions over the full range of $|t|$ in comparison with the TOTEM data at 7 TeV in Fig. 4 (a). Considering that the measurement spans 8 orders of magnitude, the match of the prediction and the measurements is fairly satisfactory. The model has some deviation from the data in the dip region, around $|t| \geq |t_{dip}| = 0.52 \text{ GeV}^2$, however this region is the most subtle one, so we leave its description to a future analysis. In the small- t region (see Fig. 4 (b)) the comparison of our predictions and the measured cross section remains fair, and the data and predictions differ by less than 10%. However we must observe that the slope of the measured cross section is higher than our prediction (see Fig. 4 (b)). Comparison of predicted values and measured ones by TOTEM are presented in Table. I. One can see that the model predicts the general trend of the data quite well. There are, however, nonnegligible deviations, in particular, the total cross section is slightly underestimated, the slope of the elastic differential cross section and $d\sigma_{el}/dt|_{t=0}$ are slightly smaller than measured values. Inelastic cross section at 7 TeV was measured by the TOTEM Collaboration Ref.[4, 6], the CMS Collaboration Ref. [7, 8], the ALICE Collaboration Ref.[9], and the ATLAS Collaboration Ref. [10] while our model prediction is $\sigma_{inelastic} = 70.34 \pm 2.11 \text{ mb}$ and $\sigma_{inelastic}/\sigma_{tot} = 0.74$ (see Table I). This ratio is close to its experimental value $\sigma_{inelastic}/\sigma_{tot} \approx 0.72$.

Given the quality of the comparison we are confident that, on the whole, our model has proved its predictive power. Detailed analysis of the impact of the TOTEM data on the parameters of the model will be presented elsewhere.

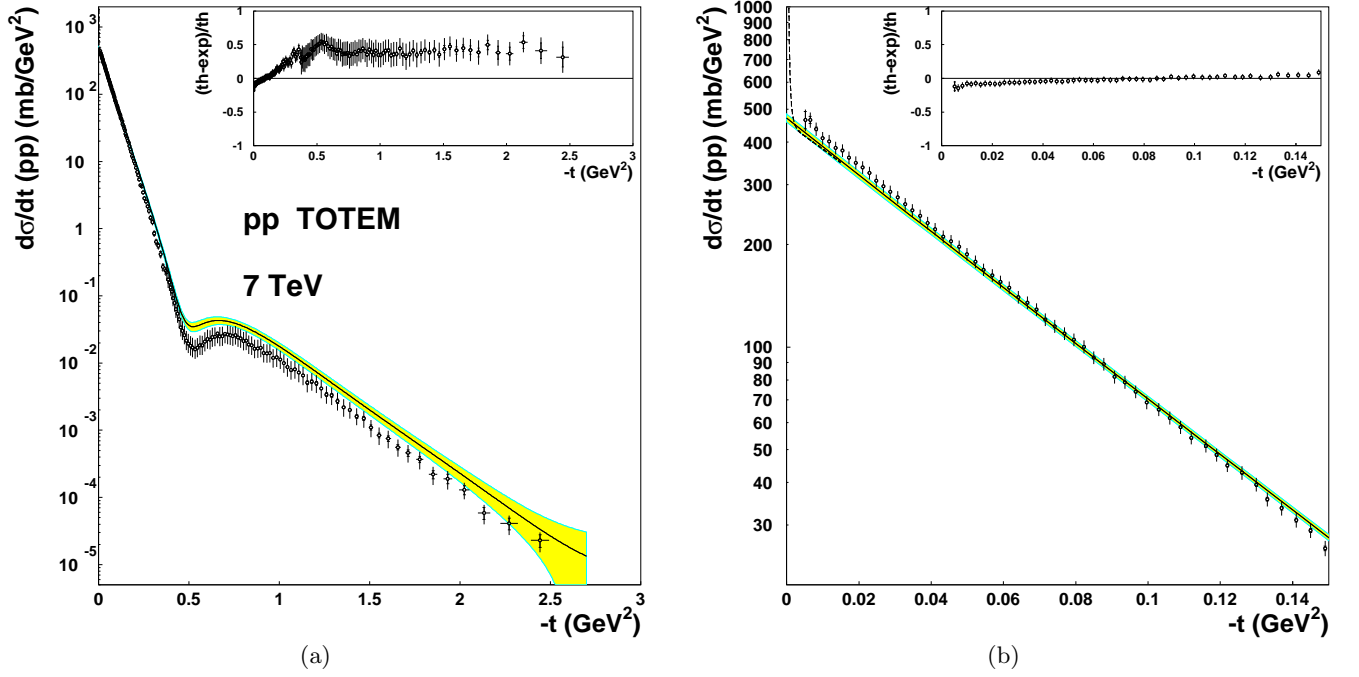


FIG. 4: Differential cross section for pp scattering at 7 TeV in comparison with the TOTEM data over whole (a) and small- t (b) regions. The yellow band corresponds to the error propagation of parameter uncertainties of the model. Upper panel shows the variance of the model predictions and the data. Cross section with coulomb-nuclear interference is shown by the dashed line in (b).

	Experimental result	Model prediction
σ_{tot} [mb], TOTEM, [6]	98.58 ± 2.23	95.06 ± 1.26
$\sigma_{elastic}$ [mb], TOTEM, [6]	25.42 ± 1.07	24.72 ± 0.85
$\sigma_{inelastic}$ [mb], TOTEM, [5]	$73.5 \pm 0.6^{+1.8}_{-1.3}$	70.34 ± 2.11
$\sigma_{inelastic}$ [mb], CMS, [8]	$64.5 \pm 3.0 \pm 1.5$	70.34 ± 2.11
$\sigma_{inelastic}$ [mb], CMS, [7]	$68 \pm 2 \pm 2.4 \pm 4$	70.34 ± 2.11
$\sigma_{inelastic}$ [mb], ATLAS, [10]	$69.4 \pm 2.4 \pm 6.9$	70.34 ± 2.11
$\sigma_{inelastic}$ [mb], ALICE, [9]	$73.2^{+2.0}_{-4.6} \pm 2.6$	70.34 ± 2.11
$d\sigma_{el}/dt _{t=0}$ [mb/GeV ²], TOTEM, [6]	506.4 ± 23.0	470.9 ± 12.5
B [mb/GeV ²] [GeV ⁻²], TOTEM, [6]	19.89 ± 0.27	19.32
$B_{(t =0.4 \text{ GeV}^2)}$ TOTEM, [GeV ⁻²], [4]	$23.6 \pm 0.5 \pm 0.5$	22.1
$ t_{dip} $ [GeV ²], TOTEM, [4]	$0.53 \pm 0.01 \pm 0.01$	0.52

TABLE I: Comparison of experimental measurement by TOTEM collaboration Ref.[4, 6], CMS Collaboration Ref. [7, 8], ALICE Collaboration Ref.[9], and ATLAS Collaboration Ref. [10] and model predictions Ref. [1] at $\sqrt{s}=7$ TeV.

CONCLUSIONS

The above analysis shows that the $D\mathcal{O}$ data [3] on the total and differential cross-sections support our predictions. Total, elastic, and inelastic cross section predictions are in agreement with the measurements by TOTEM [4, 6], CMS [7, 8], ALICE [9] and ATLAS [10]. The TOTEM [6] results on differential elastic cross-section, while being in agreement with the predictions of such general characteristics as the forward slope and the position of the dip reveal a moderate but non-negligible discrepancy with the observed t -dependence at large t . Nonetheless, the disagreement with the TOTEM [6] is, to our mind, far from being deadly. We believe that the model should be improved as, for example, in view of possible future measurements of the diffractive central production of Higgs and other states, there is a need for a good model of diffraction, whose parameters constitute an important element of the corresponding modeling. We have also to add that the very model contains, in its theoretical framework, a lot of potential sources for further refinement.

IV. ACKNOWLEDGMENTS

We are grateful to Roman Ryutin and Anton Godizov for useful discussions of the subject of this note and to Michael Pennington for critical reading of the manuscript. Authored by a Jefferson Science Associate, LLC under U.S. DOE Contract No. DE-AC05-06OR23177. The U.S. Government retains a non-exclusive, paid-up, irrevocable, world-wide license to publish or reproduce this manuscript for U.S. Government purposes.

Appendix A:

In order to estimate the error corridor of our predictions from Ref. [1] we use the following method. Generically for a measured function $f(x, \{a\})$ that depends on variable x and a set of parameters $\{a\} = \{a_1, \dots, a_N\}$, error propagation reads:

$$(\Delta f(x, \{a\}))^2 = \sum_{i=1}^N \sum_{j=1}^N C_{ij} \frac{\partial f}{\partial a_i} \sigma_i \frac{\partial f}{\partial a_j} \sigma_j, \quad (\text{A1})$$

where σ_i, σ_j are one sigma errors on parameters (in our case we use those from Table II) and C_{ij} is the correlation coefficient for parameters i and j . For totally uncorrelated parameters we have $C_{ij} = \delta_{ij}$ and the formula reduces to the standard one:

$$(\Delta f(x, \{a\}))^2 = \sum_{i=1}^N \left(\frac{\partial f}{\partial a_i} \right)^2 \sigma_i^2. \quad (\text{A2})$$

We extract the error correlation matrix from Ref. [1] and apply Eq. (A1) to all measured quantities plotted in this note.

Pomeron ₁	Odderon
$\Delta_{\mathbb{P}_1} = 0.0578 \pm 0.0020$	$\Delta_{\mathbb{O}} = 0.19200 \pm 0.0025$
$c_{\mathbb{P}_1} = 53.007 \pm 0.795$	$c_{\mathbb{O}} = 0.0166 \pm 0.0022$
$\alpha'_{\mathbb{P}_1} = 0.5596 \pm 0.0078 \text{ (GeV}^{-2}\text{)}$	$\alpha'_{\mathbb{O}} = 0.048 \pm 0.0027 \text{ (GeV}^{-2}\text{)}$
$r_{\mathbb{P}_1}^2 = 6.3096 \pm 0.2522 \text{ (GeV}^{-2}\text{)}$	$r_{\mathbb{O}}^2 = 0.1398 \pm 0.0570 \text{ (GeV}^{-2}\text{)}$
Pomeron ₂	ω -Reggeon
$\Delta_{\mathbb{P}_2} = 0.1669 \pm 0.0012$	$\Delta_{\omega} = -0.53 \text{ (FIXED)}$
$c_{\mathbb{P}_2} = 9.6762 \pm 0.1600$	$c_{\omega} = -174.18 \pm 2.72$
$\alpha'_{\mathbb{P}_2} = 0.2733 \pm 0.0056 \text{ (GeV}^{-2}\text{)}$	$\alpha'_{\omega} = 0.93 \text{ (GeV}^{-2}\text{) (FIXED)}$
$r_{\mathbb{P}_2}^2 = 3.1097 \pm 0.1817 \text{ (GeV}^{-2}\text{)}$	$r_{\omega}^2 = 7.467 \pm 1.083 \text{ (GeV}^{-2}\text{)}$
Pomeron ₃	f-Reggeon
$\Delta_{\mathbb{P}_3} = 0.2032 \pm 0.0041$	$\Delta_f = -0.31 \text{ (FIXED)}$
$c_{\mathbb{P}_3} = 1.6654 \pm 0.0669$	$c_f = 191.69 \pm 2.12$
$\alpha'_{\mathbb{P}_3} = 0.0937 \pm 0.0029 \text{ (GeV}^{-2}\text{)}$	$\alpha'_f = 0.84 \text{ (GeV}^{-2}\text{) (FIXED)}$
$r_{\mathbb{P}_3}^2 = 2.4771 \pm 0.0964 \text{ (GeV}^{-2}\text{)}$	$r_f^2 = 31.593 \pm 1.099 \text{ (GeV}^{-2}\text{)}$

TABLE II: Parameters obtained in Ref [1].

-
- [1] V.A. Petrov, A.V.Prokudin, *Eur.Phys.J. C* **23**, 135-143 (2002).
[2] V. A. Petrov, E. Predazzi and A. Prokudin, *Eur. Phys. J. C* **28**, 525 (2003) [hep-ph/0206012].
[3] V. M. Abazov *et al.* [DØ Collaboration], arXiv:1206.0687 [hep-ex].
[4] G. Antchev *et al.* [TOTEM Collaboration], *Europhys. Lett.* **95**, 41001 (2011) [arXiv:1110.1385 [hep-ex]].
[5] G. Antchev, P. Aspell, I. Atanassov, V. Avati, J. Baechler, V. Berardi, M. Berretti and E. Bossini *et al.*, *Europhys. Lett.* **96**, 21002 (2011) [arXiv:1110.1395 [hep-ex]].

- [6] G. Antchev, P. Aspell, I. Atanassov, V. Avati, J. Baechler, V. Berardi, M. Berretti and E. Bossini *et al.*, CERN-PH-EP-2012-239.
- [7] [CMS Collaboration], CMS-PAS-FWD-11-001.
- [8] [CMS Collaboration], CMS-PAS-QCD-11-002.
- [9] B. Abelev *et al.* [ALICE Collaboration], [arXiv:1208.4968 [hep-ex]].
- [10] G. Aad *et al.* [ATLAS Collaboration], Nature Commun. **2**, 463 (2011) [arXiv:1104.0326 [hep-ex]].
- [11] C. Bourrely, J. M. Myers, J. Soffer and T. T. Wu, Phys. Rev. D **85**, 096009 (2012) [arXiv:1202.3611 [hep-ph]].
- [12] J. Soffer, arXiv:1206.3657 [hep-ph].
- [13] A. Grau, S. Pacetti, G. Pancheri and Y. N. Srivastava, Phys. Lett. B **714**, 70 (2012) [arXiv:1206.1076 [hep-ph]].
- [14] O. V. Selyugin, arXiv:1205.5867 [hep-ph].
- [15] F. Nemes and T. Csorgo, arXiv:1204.5617 [hep-ph].
- [16] C. Merino and Y. M. Shabelski, JHEP **1205**, 013 (2012) [arXiv:1204.0769 [hep-ph]].
- [17] A. A. Godizov, arXiv:1203.6013 [hep-ph].
- [18] M. G. Ryskin, A. D. Martin and V. A. Khoze, Eur. Phys. J. C **72**, 1937 (2012) [arXiv:1201.6298 [hep-ph]].
- [19] V. A. Schegelsky and M. G. Ryskin, Phys. Rev. D **85**, 094024 (2012) [arXiv:1112.3243 [hep-ph]].
- [20] A. I. Lengyel and Z. Z. Tarics, arXiv:1206.5837 [hep-ph].
- [21] S. M. Troshin and N. E. Tyurin, Mod. Phys. Lett. A **27**, 1250111 (2012) [arXiv:1203.5137 [hep-ph]].
- [22] E. Gotsman, E. Levin and U. Maor, Phys. Rev. D **85**, 094007 (2012) [arXiv:1203.2419 [hep-ph]].
- [23] M. M. Block and F. Halzen, arXiv:1201.0960 [hep-ph].
- [24] A. Donnachie and P. V. Landshoff, arXiv:1112.2485 [hep-ph].
- [25] B. Z. Kopeliovich, I. K. Potashnikova and B. Povh, arXiv:1208.5446 [hep-ph].
- [26] M. M. Block and F. Halzen, Phys. Rev. D **83**, 077901 (2011) [arXiv:1102.3163 [hep-ph]].
- [27] M. M. Block and F. Halzen, Phys. Rev. Lett. **107**, 212002 (2011) [arXiv:1109.2041 [hep-ph]].
- [28] M. M. Block and F. Halzen, Phys. Rev. D **86**, 051504 (2012) [arXiv:1208.4086 [hep-ph]].
- [29] C. Bourrely, J. Soffer and T. T. Wu, Eur. Phys. J. C **28**, 97 (2003) [hep-ph/0210264].
- [30] M. M. Islam, J. Kaspar and R. J. Luddy, Mod. Phys. Lett. A **24**, 485 (2009).
- [31] L. Jenkovszky, O. Kuprash, J. Lamsa and R. Orava, Mod. Phys. Lett. A **26**, 2029 (2011) [arXiv:1106.3299 [hep-ph]].
- [32] J. Kaspar, V. Kundrat, M. Lokajicek and J. Prochazka, Nucl. Phys. B **843**, 84 (2011).
- [33] C. Lovelace, Nucl. Phys. B **95** (1975) 12.;
D. Heckathorn, Phys. Rev. D **18** (1978) 1286.;
L. N. Lipatov, Sov. Phys. JETP **63** (1986) 904-912.
- [34] O. V. Kancheli, arXiv:1105.0792 [hep-ph].
- [35] A. A. Godizov, Phys. Rev. D **81**, 065009 (2010) [arXiv:0912.1744 [hep-th]].
- [36] N. N. Nikolaev, Nucl. Phys. Proc. Suppl. **12** (1990) 95.
- [37] A. Donnachie and P. V. Landshoff, Phys. Lett. B **437**, 408 (1998) [hep-ph/9806344].
- [38] A. K. Likhoded and O. P. Yushchenko, Int. J. Mod. Phys. A **6**, 913 (1991).
- [39] J. Ellis, H. Kowalski and D. A. Ross, Phys. Lett. B **668**, 51 (2008) [arXiv:0803.0258 [hep-ph]].
- [40] V. A. Petrov, AIP Conf. Proc. **1105** (2009) 266-269.;
A. A. Godizov and V. A. Petrov, JHEP **0707** (2007) 083.
- [41] R. Kirschner and L.N. Lipatov, Z. Physik **C 45** (1990) 477.
- [42] G. B. West and D. R. Yennie, Phys. Rev. D **172**, 1413 (1968).
- [43] R. Cahn, Z. Phys. C **15**, 253 (1982).
- [44] O. V. Selyugin, Phys. Rev. D **60**, 074028 (1999).
- [45] The data are available at REACTION DATA Database <http://durpdg.dur.ac.uk/hepdata/reac.html>